## Infinite Invariant Density Determines Statistics of Time Averages for Weak Chaos

N. Korabel and E. Barkai

Department of Physics, Institute of Nanotechnology and Advanced Materials, Bar Ilan University, Ramat-Gan 52900, Israel

Weakly chaotic non-linear maps with marginal fixed points have an infinite invariant measure. Time averages of integrable and non-integrable observables remain random even in the long time limit. Temporal averages of integrable observables are described by the Aaronson-Darling-Kac theorem. We find the distribution of time averages of non-integrable observables, for example the time average position of the particle,  $\overline{x}$ . We show how this distribution is related to the infinite invariant density. We establish four identities between amplitude ratios controlling the statistics of the problem.

PACS numbers: 05.90.+m, 05.45.Ac, 74.40.De

Low dimensional chaotic systems by definition have positive Lyapunov exponents and have been extensively used to test basic assumptions of statistical physics. Weakly chaotic systems have zero Lyapunov exponents, namely the separation of trajectories is sub-exponential, though the deterministic motion remains quasi-random. In many cases discrete maps are used to model the dynamics, since they help to establish a deep understanding of the fundamental issues without being too complicated (importantly numerics converge faster than in more realistic models). In particular Pomeau-Manneville [1] maps are weakly chaotic [2] and are characterized by marginal instability. These maps were used to model intermittency [1], anomalous diffusion [3–6] and aging [7]. Such systems are described by an infinite invariant density  $(\infty D)$ [8, 9]: a non-normalizable density defined below. It is also well known that temporal averages in such systems are not equal to a corresponding ensemble average, instead time averages remain random variables even in the long measurement time limit [8, 10–13]. Since chaos is a precondition for statistical physics, it is not very surprising that weak chaos implies the breakdown of standard ergodic theory.

For an ergodic process, in the long time limit the time average of an observable is equal to the corresponding ensemble average. The ensemble average and hence the time average are obtained from the normalized invariant density, if it exists. A fundamental extension of standard ergodic theory is to find the distribution of time averages of generic observables for weakly chaotic systems where the underlying invariant density is nonnormalizable. The Aaronson-Darling-Kac (ADK) theorem [8] gives a partial answer to this problem. Briefly, an observable whose average with respect to the  $\infty D$  is finite, the distribution of properly scaled temporal averages is the Mittag-Leffler distribution. The  $\infty D$  is essential for the description of these fluctuations. For example, the separation of trajectories is described by a stretched exponential (a manifestation of weak chaos) and the distribution of separation rates is provided by the ADK theorem [14, 15].

In this manuscript, we consider the very large class of non-integrable observables. We focus on the position of

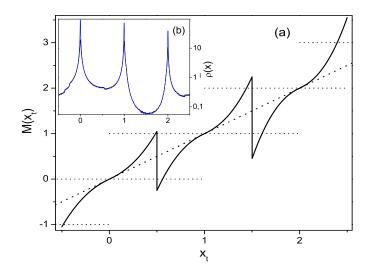


FIG. 1: (Color online) (a) The map Eq. (19) with L = 3 and  $\alpha = 3/4$  has IFPs on 0, 1, 2. (b) The  $\infty D$  exhibits non-integrable divergence on the IFPs (parameters are given in third example in the text).

a particle  $x_t$  in an interval (0, L) and obtain the distribution of its time average. Importantly we show how the distribution of time averages of non integrable observables is related to the underlying  $\infty D$ . Previously Thaler and Zweimüller [10, 11] considered an important non-integrable observable: the occupation fraction; i.e., the fraction of time the particle spends within a given domain. They rigorously showed it is described by the Lamperti distribution (see details below). We provide a very general conjecture for the distribution of time averages of non-integrable observables, without giving a rigorous proof but rather relying on simple arguments. Further we derive the identity of four amplitude ratios which govern the statistics of the problem. These identities bridge between the stochastic and dynamical theories in this field.

Model and observable. We consider measure preserv-

ing maps  $x_{t+1} = M(x_t)$  with  $x_t \in (0, L)$ . Our observable is  $x_t$  and our goal is to calculate the distribution of its time average  $\overline{x} = \sum_{t=0}^{t-1} x_t/t$ , in the limit of long time. We assume that the map has N indifferent fixed points (IFPs) located on  $\{x(1), ..., x(j), ..., x(N)\}$  such that  $M(x) \sim x + 2^{1/\alpha} a_i |x - x(j)|^{1+1/\alpha}$  as  $x \to x(j)$  and  $a_i \neq 0$ (IFPs are also called marginal fixed points). Throughout this work, j is a label of the IFPs. Here we consider  $0 < \alpha < 1$  since in that regime the distribution of  $\overline{x}$  is non-trivial. An example map is shown in Fig. 1. We consider maps where the trajectory of the particle visits the vicinity of all the IFPs; i.e., we exclude stable points or a decomposable phase space, so the transformation has an infinite invariant measure. Such maps exhibit non-Gaussian intermittency and hence have attracted vast research using various methods such as CTRW [3–5] and periodic orbit theory [6].

Power law sojourn times are related to the injection probability. Let us consider the IFP x(1) which we designate to be on the origin x(1) = 0. In the vicinity of this point the map is  $x_{t+1} \simeq x_t + 2^{1/\alpha}a_1(x_t)^{1/\alpha+1}$  for  $x_t > 0$  and  $0 < \alpha < 1$  while  $a_1 > 0$  (other IFPs have constants  $a_j$ ). Starting on  $x_0$  the time  $\tau$  it takes the particle to reach a threshold  $x_c$  is determined by the continuous approximation of the map  $dx/dt \simeq 2^{1/\alpha}a_1(x)^{1/\alpha+1}$ . Following Geisel and co-workers [3] this gives

$$\tau = \alpha \frac{(x_0)^{-1/\alpha} - (x_c)^{-1/\alpha}}{2^{1/\alpha} a_1}.$$
 (1)

During the evolution the particle is injected in the vicinity of the IFP many times and hence  $x_0$  is treated as a random variable whose probability density function (PDF) is  $P^{\text{in}}[x_0]$ . It follows that the waiting time  $\tau$ , the time the particle remains in the vicinity of the j = 1 IFP, is a random variable with the PDF  $\psi_1(\tau) =$  $P^{\text{in}}[x_0]|dx_0/d\tau|$ . A similar formula holds for the *j*th IFP. Using Eq. (1) one finds the PDF of waiting times [3]

$$\psi_j(\tau) \sim A_j \tau^{-(1+\alpha)}$$
 with  $A_j = P^{\text{in}}[x(j)] \frac{\alpha^{1+\alpha}}{2|a_j|^{\alpha}}$ . (2)

Notice that this result is independent of the threshold  $x_c$ . Here it is assumed that the injection PDF  $P^{\text{in}}[x(j)]$  is smooth in the vicinity of the IFP. Eq. (2) is well known but actually rather formal since it expresses  $\psi_j(\tau)$  in terms of the unknown injection PDF. Below we will relate the injection PDF with the  $\infty$ D. The power-law PDF Eq. (2) indicates a diverging average sojourn time since  $0 < \alpha < 1$ . The corresponding stochastic picture [3, 5] is of a particle jumping between neighborhoods of the IFPs  $\{x(1)\cdots x(N)\}$  with power law sojourn times for the trapping events.

The infinite invariant density plays a crucial role and it is defined as [16]

$$\overline{\rho}(x) \simeq \rho(x,t)/t^{\alpha-1}, \quad t \to \infty$$
 (3)

where  $\rho(x,t)$  is the density of particles [in simulations we use initial conditions uniformly spread in (0, L)]. When  $\alpha < 1$ , the invariant density is non-normalizable,  $\int_0^L \overline{\rho}(x) dx = \infty$ , and hence its name. Such  $\infty$ Ds are not common in physics though recently an application was suggested in the context of cooling in optical lattices [17]. Note that the density  $\rho(x,t)$  is, as usual, normalizable for any finite t since the maps conserve the number of particles. In the vicinity of the IFP x(j) one finds the non-integrable behavior

$$\overline{\rho}(x) \simeq b_j |x - x(j)|^{-1/\alpha}, \tag{4}$$

where  $b_j \ge 0$  is an amplitude which is generally unknown. An example  $\infty D$  is shown in Fig. 1 based on a numerical simulation which allows us to estimate the  $b_j$ s.

To understand better such a behavior we use simple arguments. Note that the density normalized to unity is

$$\rho(x,t)\mathrm{d}x \simeq t_{x,x+\mathrm{d}x}/t \tag{5}$$

where  $t_{x,x+dx}$  is the time the particle spends in (x, x+dx)[18]. Let us consider the vicinity of the first IFP x(1) = 0. The time  $t_{x,x+dx}$  is proportional to  $N_R$ : the number of injections to the vicinity of the IFPs, multiplied by  $P^{\text{in}}[x(1)]dx$  [which gives the number of visits in the interval (x, x+dx)].  $t_{x,x+dx}$  is also proportional to the time the particle stays in (x, x + dx) during each visit, which we call  $\Delta t$ . Thus, close to the IFP,

$$\rho(x,t) \simeq \frac{N_R P^{\rm in}\left[x(1)\right] \Delta t}{t}.$$
(6)

As is well known from renewal theory [3, 5] the number of renewals or injections scales like  $N_R \simeq Ct^{\alpha}$ . The pre-factor C can be roughly estimated however below we show that it is an irrelevant parameter. Using Eq. (1) we have when  $x \to 0$ 

$$\Delta t \simeq \frac{\alpha x^{-1/\alpha}}{2^{1/\alpha} a_1},\tag{7}$$

so that the closer the particle is to the IFP x(1) = 0 the longer is  $\Delta t$ . Similarly we analyze other IFPs. Putting these pieces of information together, we find

$$\rho(x,t) \simeq b_j \frac{|x-x(j)|^{-1/\alpha}}{t^{1-\alpha}} \text{ where } b_j = \frac{C\alpha P^{\text{in}}\left[x(j)\right]}{2^{1/\alpha}a_j}.$$
(8)

Eq. (8) shows, a relation between the amplitudes of the  $\infty$ Ds; i.e., the  $b_j$ s and the injection probabilities  $P^{in}[x(j)]$  [19].

The time average  $\overline{x}$  is now considered. During the evolution the trajectory of the particle  $x_t$  spends long times, of the order of the measurement time in the vicinity of the IFPs. In contrast the time it takes the particle to jump between one IFP state to another is short and can be neglected. Hence along a trajectory  $x_t$  attains observable values which are (nearly) equal to the locations of the IFP  $\{x(1)\cdots x(N)\}$ . In each one of these states the particle remains a time  $t_j$  with  $j = 1, \cdots, N$  which

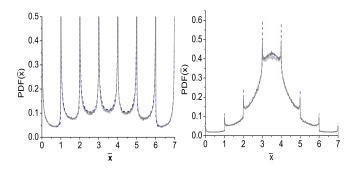


FIG. 2: (Color online) Numerical PDF of  $\overline{x}$  (solid line), perfectly matches the theory Eq. (20) (dashed line) without any fitting [map Eq. (19), left panel  $\alpha = 0.3$ , right  $\alpha = 0.75$  and  $t = 10^6$ ].

is the occupation time of state j. It follows that the time average is

$$\overline{x} \simeq \frac{\sum_{j=1}^{N} x(j) t_j}{t}.$$
(9)

Each  $t_j$  is a sum of many independent identically distributed random sojourn times drawn from the long tailed PDF  $\psi_j(\tau)$ , Eq. (2). Hence the occupation time  $t_j$ is distributed according to Lévy statistics, i.e. the generalized central limit theorem holds. More precisely  $t_j$ is a stable random variable whose PDF is the one sided Lévy function with index  $0 < \alpha < 1$ . Let  $p_j^{\text{eq}} = \langle t_j \rangle / t$ be the averaged occupation fraction treated rigorously in [10, 11] which is nothing but the probability that a member of an ensemble of noninteracting particles is in the vicinity of the IFP j. Since the occupation time  $t_j$  scale with  $A_j$  and  $t = \sum_{j=1}^N t_j$  we get

$$p_j^{\rm eq} = \frac{A_j}{\sum_{j=1}^N A_j},$$
 (10)

where  $A_j$  is the amplitude of the waiting time PDF, defined in Eq. (2). Importantly, using Eqs. (2,10),

$$p_j^{\text{eq}} = \frac{P^{\text{in}}[x(j)] |a_j|^{-\alpha}}{\sum_{j=1}^N P^{\text{in}}[x(j)] |a_j|^{-\alpha}},$$
(11)

which relates occupation fractions with injection probabilities. Using Eqs. (8,11)

$$p_j^{\text{eq}} = \frac{b_j |a_j|^{-\alpha+1}}{\sum_{j=1}^N b_j |a_j|^{-\alpha+1}},$$
(12)

which relates the occupation fractions and the  $\infty D$ .

The distribution of observables like  $\overline{x}$  was recently studied within the continuous time random walk model, a stochastic approach extensively applied, though so far without an underlying  $\infty D$ . Briefly, as mentioned,  $t_j$  is a stable random variable, and since  $\overline{x}$  [Eq. (9)] is a linear combination of such independent random variables, one finds the PDF of the time average [20]

$$f_{\alpha}(\overline{x}) = -\frac{1}{\pi} \lim_{\epsilon \to 0} \operatorname{Im} \frac{\sum_{j=1}^{N} p_{j}^{\mathrm{eq}} |\overline{x} - x(j) + i\epsilon|^{\alpha-1}}{\sum_{j=1}^{N} p_{j}^{\mathrm{eq}} |\overline{x} - x(j) + i\epsilon|^{\alpha}}, \quad (13)$$

where  $i = \sqrt{-1}$  and Im denotes the imaginary part. We see that the PDF of  $\overline{x}$  is controlled by the nonlinearity of the map in the vicinity of the IFPs, i.e.  $\alpha$ , the values of the observable on these points  $\{x(j)\}$ , the equilibrium probabilities  $p_j^{\text{eq}}$  which in turn depend on either the  $\infty$ D, Eq. (12), or the injection PDF, Eq. (11). Thus once the invariant density is known one may obtain full information on the fluctuations of the time average of our observable. Notice that when  $\alpha \to 1$ , Eq. (13) yields  $\lim_{\alpha \to 1} f_{\alpha}(\overline{x}) \sim \delta(\overline{x} - \langle x \rangle)$  where  $\langle x \rangle = \sum p_j^{\text{eq}} x(j)$ is the ensemble average. For a general non-integrable observable  $\mathcal{O}(x_t)$ , the distribution of the time average  $\overline{\mathcal{O}} = \sum_{t=0}^{t-1} \mathcal{O}(x_t)/t$  is  $f_{\alpha}(\overline{\mathcal{O}})$  as in Eq. (13) where on the right hand side we replace x(j) with  $\mathcal{O}(x(j))$ .

A first illustration will be a system with two IFPs. We consider  $x_t \in (0, 1)$  and

$$M(x_t) = \begin{cases} x_t + 2^{1/\alpha} (x_t)^{1+1/\alpha} & 0 < x_t < 1/5 \\ 1 + \frac{1/5 - x_t}{7/20} & 1/5 < x_t < 11/20 \\ x_t - 2^{1/\alpha} (1 - x_t)^{1+1/\alpha} & 11/20 < x_t < 1, \end{cases}$$
(14)

hence x(1) = 0 and x(2) = 1 are the IFPs of the map and  $|a_1| = |a_2|$ . We first concentrate on the injection PDF  $P^{\text{in}}[x]$ . We partition the map into two parts with a boundary on  $0 < x_c < 1$ . Following a trajectory we record events where the particle jumps over the boundary, either from left to right or vice versa. Each time the particle is injected into one of the domains  $x < x_c$  or  $x > x_c$  we record its landing position and thus generate a histogram which gives  $P^{\text{in}}[x]$ . Not surprisingly  $P^{\text{in}}[x]$ will depend on the choice of  $x_c$ . However, interestingly, the ratio  $P^{\text{in}}[x(1)]/P^{\text{in}}[x(2)]$  is a constant independent of the value of  $x_c$ . To understand this behavior note that according to Eq. (8) we get the amplitude ratio relation

$$b_2/b_1 = P^{\text{in}}[x(2)]/P^{\text{in}}[x(1)]$$
 (15)

and since  $b_2/b_1$  is clearly  $x_c$  independent so is the right hand side of this equation. Starting with a uniform density we evolve the system until time  $10^4$ , obtain an estimate for the  $\infty D \ \overline{\rho}(x)$ , and with it find  $b_1$  and  $b_2$ . For  $\alpha = 0.75$  we find  $b_1 = 0.075, b_2 = 0.16$  and for  $x_c = 0.5 \ P^{\text{in}}[x(1)] = 0.86$  and  $P^{\text{in}}[x(2)] = 1.86$  while  $P^{\text{in}}[x(1)] = 1.18$  and  $P^{\text{in}}[x(2)] = 2.58$  for  $x_c = 0.3$ . Hence Eq. (15) stands the numerical test. We have also verified this equation with other parameters.

After we get the amplitudes of the infinite invariant density,  $b_1$  and  $b_2$ , we may calculate  $p_1^{\text{eq}}$  and  $p_2^{\text{eq}}$  and so using Eq. (13) we find the PDF of  $\overline{x}$ 

$$f_{\alpha}\left(\overline{x}\right) = \frac{\pi^{-1}\sin\left(\pi\alpha\right)\mathcal{R}\overline{x}^{\alpha-1}\left(1-\overline{x}\right)^{\alpha-1}}{\mathcal{R}^{2}\left(1-\overline{x}\right)^{2\alpha} + \left(\overline{x}\right)^{2\alpha} + 2\mathcal{R}\cos\pi\alpha\left(1-\overline{x}\right)^{\alpha}\overline{x}^{\alpha}},\tag{16}$$

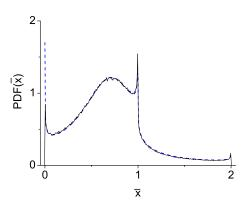


FIG. 3: (Color online) Numerical simulations give the PDF of  $\overline{x}$  (solid line) that matches the analytical density (dashed line) Eq. (13) [map Eq. (19),  $t = 10^6$ , L = 3 and  $\alpha = 3/4$ ].

which is the Lamperti PDF. The same distribution was previously obtained for the occupation fraction [10–12]. As pointed out by Akimoto [13] this is not surprising since both observables are identical on the *IFPs* [for the occupation fraction the observable is the step function which is 1 on x(2) = 1 and zero on x(1) = 0]. The parameter  $\mathcal{R}$  is

$$\mathcal{R} = \frac{A_2}{A_1} = \frac{P^{\text{in}}[x(2)]}{P^{\text{in}}[x(1)]} = \frac{b_2}{b_1} = \frac{p_2^{\text{eq}}}{p_1^{\text{eq}}}.$$
 (17)

Hence one has four amplitude ratios related to the waiting times, the injection probabilities, the  $\infty D$  and the population probabilities which determine the PDF of  $\overline{x}$ . *Amplitude ratios* can be easily generalized for the case of N IFPs and for the case where the  $a_i$ s are not all equal

$$\frac{p_j^{\text{eq}}}{p_i^{\text{eq}}} = \frac{A_j}{A_i} = \frac{|a_j|^{-\alpha} P^{\text{in}}[x(j)]}{|a_i|^{-\alpha} P^{\text{in}}[x(i)]} = \frac{b_j |a_j|^{-\alpha+1}}{b_i |a_i|^{-\alpha+1}}.$$
 (18)

The second illustration concerns maps with N degenerate IFPs. We consider N = 2L with L = 8 and  $x_t \in (-1/2, 7.5)$ . The map is

$$M(x_t) = x_t + \begin{cases} 2^{1/\alpha} \tilde{a}_k (x_t - k)^{1+1/\alpha} & k < x_t < k + 1/2 \\ -2^{1/\alpha} \tilde{a}_k (-x_t + k)^{1+1/\alpha} & k - 1/2 < x_t < k \end{cases}$$
(19)

where  $k = 0, \dots, L-1$ . Here 16 IFPs are on  $\{x(1) = 0^-, x(2) = 0^+, \dots, x(15) = 7^-, x(16) = 7^+\}$ . We use periodic boundary conditions: if  $x_t > 7.5$  or  $x_t < -1/2$  we transform  $x_t$  to  $x_t - 8$  or  $x_t + 8$  respectively. We set all  $\tilde{a}_k = 1$ . Then from symmetry we expect that all

the amplitudes  $b_j$  will be identical. It then follows that  $p_j^{\text{eq}} = 1/(2L)$ . For this degenerate case we get

$$f_{\alpha}\left(\overline{x}\right) = -\frac{1}{\pi} \lim_{\epsilon \to 0} \operatorname{Im} \sum_{j=0}^{L-1} \frac{\left(\overline{x} - j + i\epsilon\right)^{\alpha-1}}{\left(\overline{x} - j + i\epsilon\right)^{\alpha}}.$$
 (20)

Thus due to symmetry the distribution of  $\overline{x}$  depends only on a single parameter which is  $\alpha$ . In Fig. 2 we show the PDF of  $\overline{x}$  obtained numerically together with theory Eq. (20). For  $\alpha = 0.3$  the distribution is wider than the case  $\alpha = 3/4$  since we expect that as  $\alpha \to 1$  the fluctuations will vanish. Notice that  $f_{\alpha}(\overline{x})$  diverges on the IFPs reflecting trajectories with a trapping time of the order of the measurement time on one of these points.

The third example is the map Eq. (19) with L = 3and hence IFPs are on  $x(1) = 0^-, x(2) = 0^+, x(3) =$  $1^-, x(4) = 1^+, x(5) = 2^-, x(6) = 2^+$ . It follows that in the long time limit  $\overline{x} \in (0, 2)$ . We use  $\tilde{a}_1 = 1.1$ ,  $\tilde{a}_2 = 1.5$ and  $\tilde{a}_3 = 2.1$ . We numerically obtain the  $\infty$ D for  $\alpha = 3/4$ and estimate  $b_1 = b_2 \simeq 0.059, b_3 = b_4 \simeq 0.04, b_5 = b_6 \simeq$ 0.018. Inserting these values in Eq. (12) we find:  $p_1^{eq} =$  $p_2^{eq} = 0.239, p_3^{eq} = p_4^{eq} = 0.175$  and  $p_5^{eq} = p_6^{eq} = 0.086$ . This is compared with direct numerical computation of the occupation fraction:  $p_1^{eq} = p_2^{eq} \simeq 0.242, p_3^{eq} = p_4^{eq} \simeq$  $0.167, p_5^{eq} = p_6^{eq} \simeq 0.091$ . Deviations between the two methods are related to the divergence of the  $\infty D$  next to IFPs which induces errors in the estimation of the  $b_j$ s. Inserting the latter values of  $p_j^{eq}$  sinto Eq. (13) we obtain the PDF of  $\overline{x}$  which as shown in Fig. 3 perfectly matches direct numerical simulation.

Discussion. We obtained the distribution of time averages of non-integrable observables for systems with IFPs with an infinite invariant measure. The  $\infty D$ , the occupation fractions, the injection probabilities, and the amplitudes  $A_i$  of the scale free distributions of the sojourn times, are all related and can be used to determine the non-trivial distribution of the temporal averages. There exists a vast number of physical systems with dynamics governed by power law trapping times similar to the maps under investigation. A fundamental experimental question is whether such systems, e.g. blinking quantum dots [21], two dimensional rotating flows [22, 23] and electrohydrodynamic convection in liquid crystals [24] possess an infinite invariant measure. Hence it would be interesting to extract the invariant density from the trajectories in such experiments. If it is of infinite measure, one could then use our theory to predict the distribution of the temporal averages.

**Acknowledgement** This work was supported by the Israel Science Foundation.

 Y. Pomeau, and P. Manneville, Commun. Math. Phys. 74, 189 (1980); P. Manneville, J. Phys. 41, 1235 (1980).
 P. Gaspard, and X.-J. Wang, Proc. Nat. Acad. Sci. USA, **85**, 4591 (1988).

[3] T. Geisel, and S. Thomae, Phys. Rev. Lett. 52, 1936 (1984).

- [4] T. Geisel, J. Nierwetberg and A. Zacherl, Phys. Rev. Lett. 54, 616 (1985).
- [5] G. Zumofen, and J. Klafter, Phys. Rev. E. 47, 851 (1993).
- [6] R. Artuso, P. Cvinatović, and G. Tanner, Prog. Theor. Phys. Supl. 150, 1 (2003).
- [7] E. Barkai, Phys. Rev. Lett. 90, 104101 (2003).
- [8] J. Aaronson, An Introduction to Infinite Ergodic Theory, (American Mathematical Society, 1997).
- [9] S. Tasaki, and P. Gaspard, J. of Statistical Physics 109 803 (2002).
- [10] M. Thaler, Ergod. Th. & Dynam. Sys. 22, 1289 (2002).
- [11] M. Thaler, and R. Zweimuller, Probab. Theory Relat. Fields 135, 15 (2006).
- [12] G. Bel, and E. Barkai, Europhysics Lett. 74 12 (2006).
- [13] T. Akimoto, J. Stat. Phys. **132**, 171 (2008).
- [14] N. Korabel, and E. Barkai, Phys. Rev. Lett. **102**, 050601 (2009). ibid, Phys. Rev. E. **82**, 016209 (2010).
- [15] T. Akimoto, and Y. Aizawa, Chaos **20**, 033110 (2010).
- [16] In the literature the  $\infty D$  is unique up to a multiplicative constant. Our definition Eq. (3) is a convenient choice. Multiplying the  $\infty D$  with a constant does not alter our

main results, since they depend on ratios of amplitudes.

- [17] D. A. Kessler, and E. Barkai, Phys. Rev. Lett. 105, 120602 (2010).
- [18] Strictly this time is random for a given trajectory and we mean an averaged time.
- [19] Note that for any finite long time the non-integrable behavior is cut off [14]. Still, as we show in the text, the non-normalized density plays a crucial role in the determination of the distribution of the time averages through the  $b_j$ s.
- [20] A. Rebenshtok and E. Barkai, Phys. Rev. Lett. 99, 210601 (2007). ibid J. Stat. Phys. 133, 565 (2008).
- [21] F. D. Stefani, J. P. Hoogenboom, and E. Barkai, Phys. Today 62, 34 (2009).
- [22] T. H. Solomon, E. R. Weeks, and H. L. Swinney, Phys. Rev. Lett. 71, 3975 (1993).
- [23] D. del-Castillo-Negrete, Phys. of Fluids 10, 576 (1998).
- [24] L. Silvestri, L. Fronzoni, P. Grigolini, and P. Allegrini, Phys. Rev. Lett. **102**, 014502 (2009).